

# Time evolution of the approximate and stationary solutions of the Time-Fractional Forced-Damped-Wave equation

A. M. A. El-Sayed<sup>1</sup>, E. A. Abdel-Rehim<sup>2,\*</sup> and A. S. Hashem<sup>3</sup>

<sup>1</sup>Faculty of Science, Alexandria University, Alexandria, Egypt

<sup>2,3</sup>Faculty of Science, Suez Canal University, Ismailia, Egypt

\*Corresponding author

E-mail: amasayed@gmail.com<sup>1</sup>, entsarabdelrehim@yahoo.com<sup>2</sup>, amelhashem2006@yahoo.com<sup>3</sup>

## Abstract

In this paper, the simulation of the time-fractional-forced-damped-wave equation (the diffusion advection forced wave) is given for different parameters. The common finite difference rules beside the backward Grünwald–Letnikov scheme are used to find the approximation solution of this model. The paper discusses also the effects of the memory, the internal force (resistance) and the external force on the travelling wave. We follow the waves till they reach their stationary waves. The Von-Neumann stability condition is also considered and discussed. Besides the simulation of the time evolution of the approximation solution of the classical and time-fractional model, the stationary solutions are also simulated. All the numerical results are compared for different values of time.

2010 Mathematics Subject Classification. **26A33**. 35L05, 35J05, 45K05, 60J60, 60G50, 60G51, 65N06, 42A38

Keywords. approximation solution, diffusion wave equation, explicit scheme, Grünwald–Letnikov scheme, time fractional, stability, stationary solution, simulation.

## 1 Introduction

Different versions of the wave equation have been used to model acoustic absorption, dispersion in biological tissue, ultrasound wave and other huge numbers of natural phenomena. This subject has gotten a great interest among researchers over the last decade. We begin with the traditional Cauchy wave equations that models a vibrating string of length  $L$ , in an ideal medium, namely

$$\frac{\partial^2 u(x, t)}{\partial t^2} = a \frac{\partial^2 u(x, t)}{\partial x^2}, \quad -R \leq x \leq R, \quad t > 0, \quad L = 2R + 1, \quad (1.1)$$

where  $u(x, t)$  represents the vertical displacement of the vibration, and  $a > 0$  is a general positive constant of diffusion.  $u(x, t)$  is imposed to the initial condition  $u(x, 0) = f(x)$ , and to the boundary conditions  $u(-R, t) = u(R, t) = 0$ , i.e. the string is initially fixed at its ends. One needs another initial condition to solve this equation, namely  $u_t(x, 0) = g(x)$ . This equation does not model a vibrating string but also it models many physical and biological phenomena, such as a wave propagation of sound travelling in a fluid, in a gas, or in any other ideal medium. Also it models an electrical signal travelling along transmitted cable. If the string is pushed with an external force  $F(x)$ , then this equation takes the form

$$\frac{\partial^2 u(x, t)}{\partial t^2} = a \frac{\partial^2 u(x, t)}{\partial x^2} - \frac{\partial}{\partial x}(F(x)u(x, t)). \quad (1.2)$$

This equation models a wide range of physical phenomena. For example the motion of the internal waves which occur throughout the atmosphere and oceans under the action of external forces such as pressures and thermodynamic effects. It has gotten an increasingly interests among researchers, see for example [21] and [17]. Taking under consideration the friction coefficient from an effecting resistance source with friction coefficient  $k > 0$ , one can write equation (1.2) in the form

$$\frac{\partial^2 u(x, t)}{\partial t^2} = k \frac{\partial u(x, t)}{\partial t} + a \frac{\partial^2 u(x, t)}{\partial x^2} - \frac{\partial}{\partial x}(F(x)u(x, t)), \quad t > 0. \quad (1.3)$$

This equation is called the *forced-damped wave equation*. Some mathematical researchers prefer to call it *diffusion advection wave equation*. In some situations, when discussing the electrical signal travelling along transmission cable, the term  $k \frac{\partial u(x, t)}{\partial t}$  is called the internal resistance of the wires comprising the transmission lines. In that case, the model is represented mathematically by the so called telegraph equation, see [6], [18], [24] and [28]. The over diagnostic ultrasound frequencies, acoustic absorption in biological tissue, exhibit a power law with a non integer frequency, see [10] and [7]. Also, in a complex inhomogeneous conducting medium experimental evidence shows that the sound waves propagate with power law of non integer orders. To model mathematically such problems, one has to replace the second order time derivative at equation (1.3) by the Liouville–Caputo [9] time-fractional derivative operator of order  $\beta$ , namely

$$D_{t*}^{\beta} u(x, t) = k \frac{\partial u(x, t)}{\partial t} + a \frac{\partial^2 u(x, t)}{\partial x^2} - \frac{\partial}{\partial x}(F(x)u(x, t)), \quad a > 0, k > 0. \quad (1.4)$$

For  $0 < \beta < 1$ , equation(1.4 ) represents the time-fractional diffusion under the action of an internal friction and an external force and for  $1 < \beta < 2$ , it models the time-fractional forced damped wave. For further applications on physics and on real phenomena, see [16], [20] and [26]. The Liouville–Caputo time fractional derivative operator of order  $\beta$  is defined as

$$D_{t*}^{\beta} f(t) = \begin{cases} \frac{1}{\Gamma(m-\beta)} \left\{ \int_0^t f^{(m)}(\tau) K_{\beta}(t-\tau) d\tau \right\} & \text{for } m-1 < \beta < m, \\ \frac{d^m}{dt^m} f(t) & \text{for } \beta = m, \end{cases} \quad (1.5)$$

with

$$K_{\beta}(t-\tau) = \frac{(t-\tau)^{\beta+1-m}}{\Gamma(m-\beta)},$$

being called the memory function. This kernel enables us to reflect the memory effects of many physical processes, see [9] and [27]. Trials have been done to solve this equation most of them are based on the iterative methods which give hardly approximation solutions which are not valid on the long run. Most of these trials are to find solution of equation (1.4) without external and internal forces. For example: Stojanovic [25] used an approximation method based on Laguerre polynomials to find a numerical solution to the diffusion wave equation. Agrawal [4] discussed the general analytical solution for the fourth-order fractional diffusion-wave equation. Later, the same author [5] used the sine transform technique to convert the fractional differential equation from a space domain to a wave number domain. Mainardi et al. [22] gave the fundamental solution (the green functions) of the Cauchy and signaling problems governing the time-fractional wave equation. Gorenflo et al. [12] discussed a mapping between solutions of the space-time fractional diffusion

equations and the space-time fractional wave equations. The authors have given the solutions in terms of the Green function in the form of convergent series. Elsayed et al also studied the fractional order diffusion and wave equations with numerical examples, see [11] and [15]. The signaling problem for equation (1.4) without external and internal forces, is also solved using the Laplace-Fourier transform in a half plane, see [23].

Our main goal in this paper is to simulate the approximate solution of equation (1.4) obtained by using the common finite difference rules beside using the backward Grünwald- Letnikov scheme. The Grünwald-Letnikov scheme has been used successfully, see [13], [1], [14],[2], [3] and the reference therein. The paper discusses also the effect of the memory on the travelling wave. Constantinescu et al. [8] discussed the long range memory modelling techniques on fractal dynamic systems. So far, the paper is organized as follows: section 1 is devoted to the introduction. Section 2, is to introduce the discretization of the classical forced damped wave equation and the proof of the stability of its difference scheme. In section 3, we discuss the finite difference scheme of the time-fractional forced wave equation with damping and to give the proof of its stability too. Section 4 is to find the approximate and analytical stationary solutions for this model. Finally section 5, is devoted to simulate the propagation of the waves of the previous model for different values of the parameters  $\beta$ ,  $k$ ,  $f(x)$  and  $t$ . Also, we interpret our numerical results with investigating the effect of the memory on the propagation of the waves by comparing all the results. The stationary solution for this model is also simulated and compared.

## 2 Discretization of the classical forced wave equation with damping

To find the finite difference scheme of equation (1.3), one has to identify firstly the used external force  $F(x)$ . There are many forms of  $F(x)$  which can be used depending on the kind of the model. In this paper, we derive  $F(x)$  from the potential  $U(x)$  as  $F(x) = -\frac{dU(x)}{dx}$ , where  $U(x)$  must be a symmetric differentiable potential and strictly increasing for  $x > 0$ . As an example, we consider here the quadratic harmonic oscillator  $U(x) = \frac{bx^2}{2}$ ,  $b > 0$ . Therefore,  $F(x)$  is a linear attractive force. To discretize the classical forced wave equation with damping, equation (1.3), we utilize the symmetric difference in space forward in time. So far, the space variable  $x$  is discretized by the grid points

$$x_j = jh, \quad h > 0, \quad j \in \mathbb{Z}, \quad (2.1)$$

where,  $j$  is restricted by  $j \in [-R, R]$ ,  $h = 1/(2R + 1)$ . Adjust  $\tau$  such that

$$t_n = n\tau, \quad \tau > 0, \quad n \in \mathbb{N}_0. \quad (2.2)$$

Introduce the clump  $y_j^{(n)}$  to approximate the integral of the displacement function  $u(x, t)$  over the small interval  $h$ . Then constitute the vector

$$y^{(n)} = \{y_{-R}^{(n)}, y_{-R+1}^{(n)}, \dots, y_{R-1}^{(n)}, y_R^{(n)}\}^T,$$

with a suitably initial value  $y^{(0)}$  being obtained by the aid of initial condition  $u(x, 0) = f(x)$ . Solving equation (1.3) for  $y_j^{(n+1)}$ , to get

$$y_j^{(n+1)} = \frac{-1}{1 - k\tau} y_j^{(n-1)} + \frac{2 - k\tau - 2a\mu}{1 - k\tau} y_j^{(n)} + \frac{a\mu}{1 - k\tau} \left(1 + \frac{j+1}{R}\right) y_{j+1}^{(n)} + \frac{a\mu}{1 - k\tau} \left(1 - \frac{j-1}{R}\right) y_{j-1}^{(n)} + O(\tau^2, h^2), \quad (2.3)$$

where  $R = \frac{2a}{bh^2}$  is a positive integer number, i.e.  $R \in \mathbb{Z}$  and  $\mu = \frac{\tau^2}{h^2}$  being called the scaling relation. The coefficients of  $y_j^{(n)}$  must be positive, therefore the condition imposed on  $\mu$  is

$$0 < \mu \leq \frac{1}{2a} . \quad (2.4)$$

Physical experiments show that the internal (resistance) coefficients must not increase than one. Therefore, for stability, the friction coefficient  $k$  must satisfy the condition

$$0 < k \leq 1 . \quad (2.5)$$

Our numerical results show that if  $k > 1$ , the wave damped so rapidly and reach its final stationary solution so fast. Equation (2.3) is equivalent to

$$y_j^{(n+1)} = \frac{-1}{1-k\tau} y_j^{(n-1)} + p_{jj} y_j^{(n)} + p_{j,j-1} y_{j-1}^{(n)} + p_{j,j+1} y_{j+1}^{(n)} . \quad (2.6)$$

Here  $y_j^{(n+1)}$  is interpreted as the probability of finding the particle at the point  $x_j$  at the time instant  $t_{n+1}$ ,  $n \geq 1$ . While the coefficients  $p_{j,j-1}$ ,  $p_{jj}$ ,  $p_{j,j+1}$  represent the transition probabilities from the points  $x_{j-1}$ ,  $x_j$  or  $x_{j+1}$  at the time instant  $t_n$  to the point  $x_j$  at the time instant  $t_{n+1}$  and the factor  $|\frac{-1}{1-k\tau}|$  is also a transition probability from the point  $x_j$  at the time instant  $t_{n-1}$  to  $x_j$  at the time instant  $t_{n+1}$ . One can easily prove that the summation of these transition probabilities (coefficients) is one. So far, equation (2.3) can be written in the matrix form

$$y_j^{(n+1)} = \frac{-1}{1-k\tau} y_j^{(n-1)} + P^\top \cdot y_j^{(n)} , \quad (2.7)$$

where  $P$  is a tri-diagonal matrix whose its elements  $p_{i,j} \geq 0$ , and is defined as

$$P_{ij} = \begin{cases} P_{ij}^{(1)} = \frac{a\mu}{1-k\tau} (1 - \frac{j}{R}) & j = i + 1, i = -R, \dots, R - 1 \\ P_{ij}^{(2)} = \frac{2-k\tau-2a\mu}{1-k\tau} & j = i, i = -R, \dots, R \\ P_{ij}^{(3)} = \frac{a\mu}{1-k\tau} (1 + \frac{j}{R}) & j = i - 1, i = -R + 1, \dots, R - 1 . \end{cases} \quad (2.8)$$

For the numerical computation, we introduce the row vector  $z^{(n)} = (y^{(n)})^T$ , and the matrix  $H = h_{ij}$ , where  $-R \leq i, j \leq R$ , to write equation (2.7) in the matrix form

$$z^{(n+1)} = \frac{-1}{1-k\tau} z^{(n-1)} + z^{(n)} \cdot (\frac{2-k\tau}{1-k\tau} I + \frac{\mu}{1-k\tau} H) . \quad (2.9)$$

Here  $H$  is a tri-diagonal matrix satisfying that the summation of its rows is zero. Let  $S_0 = \sum_{j=-R}^R y_j^{(0)}$

and  $S_n = \sum_{j=-R}^R y_j^{(n)}$ ,  $n \geq 1$ , and we suitably choose  $f(x)$  such that  $S_0 = 1$ . scheme (2.3) is conservative and hence forth is stable, if  $S_0 = S_n$ ,  $\forall n \geq 1$ , which is an easy task and can be proved by using equations (2.7) and (2.8) as

$$S_n = \frac{-1}{1-k\tau} + \sum_{m=1}^3 P_{ij}^{(m)} = 1 .$$

This is the proof of the stability according to *Lax-Richtmyer*, see [19]. There is another proof for the stability, namely the *Von Neumann* necessary condition for stability. The Von Neumann stability analysis is local in the sense that it does not take into account the boundary effects. It is assumed that at each grid points

$$y_j^{(n)} = \zeta^{(n)} e^{i\kappa x_j}, \quad (2.10)$$

where  $\zeta = \zeta(\kappa)$  is a complex number. The approximation solution  $y^{(n)}$  is stable if the amplification factor  $|\zeta|^2 \leq 1$ . Since there are no conditions imposed on the constants  $a$  and  $b$ , then for simplicity we put  $a = b = 1$ . After that, substitute equation (2.10) into equation (2.3), to get the following quadratic equation

$$\zeta^2 - \left( \frac{2 - k\tau - 2\mu}{1 - k\tau} + \frac{\mu}{1 - k\tau} \left( 2 \left( 1 + \frac{1}{R} \right) \cos \kappa h - \frac{2ij}{R} \sin \kappa h \right) \right) \zeta + \frac{1}{1 - k\tau} = 0. \quad (2.11)$$

By taking the limit  $h \rightarrow 0$ , one gets  $\cos \kappa h \approx 1$  and  $\sin \kappa h \approx \kappa h$ . After mathematical manipulation, equation (2.11) is rewritten as

$$\zeta^2 - \frac{1}{1 - k\tau} (2 - k\tau + (1 - ij\kappa h)\tau^2) \zeta + \frac{1}{1 - k\tau} = 0. \quad (2.12)$$

This quadratic equation has two solutions

$$\zeta_1 = \frac{(-2 + k\tau - \tau^2 + ij\kappa h\tau^2) - \sqrt{4(-1 + k\tau) + (-2 + k\tau - \tau^2 + ij\kappa h\tau^2)^2}}{2(k\tau - 1)},$$

and

$$\zeta_2 = \frac{(-2 + k\tau - \tau^2 + ij\tau^2) + \sqrt{4(-1 + k\tau) + (-2 + k\tau - \tau^2 + ij\kappa h\tau^2)^2}}{2(k\tau - 1)}.$$

By using equations (2.4,2.5) and taking the limit as  $\tau \rightarrow 0$  and  $h \rightarrow 0$ , one gets  $|\zeta_1|^2 \leq 1$  and  $|\zeta_2| \gg 1$ . Therefore,  $\zeta_2$  is ignored. So far, according to Von Neumann stability condition the difference scheme (2.3) is stable.

### 3 Discretization of the time-fractional forced wave equation with damping

In this section, the discretization of the time-fractional forced wave equation with damping is given. For this task, we replace the external force in equation (1.4), by the linear attractive force  $F(x) = -bx$ , to get

$$D_{t*}^{\beta} u(x, t) = k \frac{\partial u(x, t)}{\partial t} + a \frac{\partial^2 u(x, t)}{\partial x^2} + \frac{\partial}{\partial x} (bxu(x, t)), \quad 1 < \beta < 2, \quad x \in [-R, R], \quad (3.1)$$

with  $0 \leq t \leq T$ . This equation is imposed to the same previously used initial conditions  $u(x, 0) = f(x)$  and  $u_t(x, 0) = g(x)$ , and to the same used boundary conditions  $u(-R, t) = u(R, t) = 0$ , to be able to compare the numerical results of the two models. The Liouville-Caputo time-fractional operator  $D_{t*}^{\beta} u(x, t)$  is discretized by the Grünwald-Letnikov scheme, see [13], [1], [14] and the references therein, namely

$$D_{\tau*}^{\beta} y_j(t_{n+1}) = \sum_{m=0}^{n+1} (-1)^m \binom{\beta}{m} \frac{y_j(t_{n+1-m}) - y_j(t_0)}{\tau^{\beta}}, \quad 1 < \beta \leq 2 \quad \forall n \in N_0. \quad (3.2)$$

Observing that  $D_{\tau}^1 y_j(t_{n+1}) = \frac{1}{\tau}(y_j(t_{n+2}) - y_j(t_n))$ . Substitute equation (3.2) in equation (3.1) and use the common finite difference rules, then solve for  $y_j^{(n+1)}$ , to get

$$y_j^{(n+1)} = \frac{1}{1 - k\tau^{\beta-1}} \sum_{m=0}^n (-1)^m \binom{\beta}{m} y_j^{(0)} + \frac{1}{1 - k\tau^{\beta-1}} \sum_{m=2}^n (-1)^{m+1} \binom{\beta}{m} y_j^{(n+1-m)} +$$

$$\left( \frac{\beta - k\tau^{\beta-1} - 2\mu}{1 - k\tau^{\beta-1}} \right) y_j^{(n)} + \frac{\mu}{1 - k\tau^{\beta-1}} \left( 1 + \frac{j+1}{R} \right) y_{j+1}^{(n)} + \frac{\mu}{1 - k\tau^{\beta-1}} \left( 1 - \frac{j-1}{R} \right) y_{j-1}^{(n)} +$$

$$O(\tau^\beta, h^2) . \quad (3.3)$$

Here, the scaling relation  $\mu$  is defined as  $\mu = \frac{\tau^\beta}{h^2}$  and it must satisfy the condition

$$\mu \leq \frac{\beta - k\tau^{\beta-1}}{2} . \quad (3.4)$$

For further calculations, it is better to introduce the two parameters,  $b_n$  and  $c_m$ , namely

$$b_n = \sum_{m=0}^n (-1)^m \binom{\beta}{m} ,$$

$$c_m = (-1)^{m+1} \binom{\beta}{m} , m \geq 1 ,$$

where they have been originally introduced in [13] with  $b_0 = c_1 = \beta$ , and all  $c_k \geq 0$ ,  $b_n \geq 0$ . Finally,  $b_n$  and  $c_m$  satisfy the relation

$$b_n + \sum_{m=1}^n c_m = 1 . \quad (3.5)$$

Equation (3.3) is equivalent to

$$y_j^{(n+1)} = \frac{1}{1 - k\tau^{\beta-1}} b_n y_j^{(0)} + \frac{1}{1 - k\tau^{\beta-1}} \sum_{m=2}^n c_m y_j^{(n+1-m)} +$$

$$q_{j,j} y_j^{(n)} + q_{j,j-1} y_{j-1}^{(n)} + q_{j,j+1} y_{j+1}^{(n)} . \quad (3.6)$$

Again,  $y_j^{(n+1)}$  is interpreted as the probability of finding the particle at the point  $x_j$  at the time instant  $t_{n+1}$ ,  $n \geq 1$ . While the coefficients  $q_{j,j-1}$ ,  $q_{j,j}$ ,  $q_{j,j+1}$  represent the transition probabilities from the points  $x_{j-1}$ ,  $x_j$  or  $x_{j+1}$  at the time instant  $t_n$  to the point  $x_j$  at the time instant  $t_{n+1}$ . The coefficients  $c_m$ ,  $2 \leq m < n$  are the transition probabilities from  $x_j$  at the time instants  $t_{n-2}, \dots, t_1$  to  $x_j$  at  $t_{n+1}$  while  $b_n$  is the transition probability from  $x_j$  at  $t_0$  to  $x_j$  at  $t_{n+1}$ . Equation (3.3) is now written in the following matrix form

$$y^{(n+1)} = \frac{1}{1 - k\tau^{\beta-1}} b_n y^{(0)} + \frac{1}{1 - k\tau^{\beta-1}} \sum_{m=2}^n c_m y^{(n+1-m)} + Q^T \cdot y^{(n)} , \quad (3.7)$$

where, the matrix  $Q = q_{ij}$ ,  $i, j \in [-R, R]$  has the form

$$q_{ij} = \begin{cases} q_{ij}^{(1)} = \frac{\mu}{1-k\tau^{\beta-1}} \left(1 - \frac{j}{R}\right) & j = i + 1, i = -R, \dots, R - 1 \\ q_{ij}^{(2)} = \frac{\beta - k\tau^{\beta-1} - 2\mu}{1 - k\tau^{\beta-1}} & j = i, i = -R, \dots, R \\ q_{ij}^{(3)} = \frac{\mu}{1 - k\tau^{\beta-1}} \left(1 + \frac{j}{R}\right) & j = i - 1, i = -R + 1, \dots, R - 1. \end{cases} \quad (3.8)$$

By using the same previously used vector  $z^{(n)}$ , equation (3.7) is rewritten as

$$z^{(n+1)} = \frac{1}{1 - k\tau^{\beta-1}} b_n z^{(0)} + \frac{1}{1 - k\tau^{\beta-1}} \sum_{m=2}^n c_m z^{(n+1-m)} + z^{(n)}.Q. \quad (3.9)$$

By using the same defined matrix  $H$ , equation (3.9) is rewritten as

$$z^{(n+1)} = \frac{1}{1 - k\tau^{\beta-1}} b_n z^{(0)} + \frac{1}{1 - k\tau^{\beta-1}} \sum_{m=2}^n c_m z^{(n+1-m)} + z^{(n)}. \left( \frac{\beta - k\tau^{\beta-1}}{1 - k\tau^{\beta-1}} I + \frac{\mu}{1 - k\tau^{\beta-1}} H \right). \quad (3.10)$$

One can easily prove that  $S_n = S_0 \forall n \geq 1$ , by the aid of equation (3.5). Therefore, the discretization equation (3.3) is stable according to *Lax-Richtmyer*, see [19]. The time-fractional approximation solution,  $y^{(n+1)}$  depends not only on  $y_{j-1}^{(n)}$ ,  $y_j^{(n)}$ ,  $y_{j+1}^{(n)}$ , but also on  $y_j^{(n-1)}$ ,  $y_j^{(n-2)}$ ,  $\dots$  and back to  $y_j^{(0)}$ . That means the approximation solution of the time-fractional forced wave equation with damping depends on the history of the system, i.e. the process has a memory. This memory has a concrete effects on the evaluation of the dynamic behavior of the model being under discussion. The other proof of the stability namely, the *Von Neumann* necessary condition for stability is difficult as in this case  $y^{(n+1)}$  depends on all its history. Therefore to prove the stability, one has to do it on steps. Firstly, we ignore the coefficients of  $y^{(n-1)}$ ,  $y^{(n-2)}$ ,  $\dots$ ,  $y^{(0)}$ , and substitute equation (2.10) on the rest of equation (3.3), to get after manipulations

$$\zeta = \left( \frac{\beta - k\tau^{\beta-1}}{1 - k\tau^{\beta-1}} + \frac{2\mu}{R(1 - k\tau^{\beta-1})} \right) \cos(\kappa j h) + \frac{2i\mu}{R(1 - k\tau^{\beta-1})} \sin(\kappa j h). \quad (3.11)$$

By using the stability condition (2.5) and taking the limits as  $h \rightarrow 0$  and  $\tau \rightarrow 0$ , one gets  $|\zeta|^2 < 1$ . Secondly, we take into consideration the dependence of  $y^{(n+1)}$  on  $y^{(n)}$  and  $y^{(n-1)}$ , only, to get after calculations

$$\zeta^2 - \left( \frac{\beta - k\tau^{\beta-1} - 2\mu}{1 - k\tau^{\beta-1}} + \frac{\mu}{1 - k\tau^{\beta-1}} \left(1 + \frac{j+1}{R}\right) e^{i\kappa j h} + \frac{\mu}{1 - k\tau^{\beta-1}} \left(1 - \frac{j-1}{R}\right) e^{-i\kappa j h} \right) \zeta - \frac{\beta(\beta-1)}{2(1 - k\tau^{\beta-1})} = 0. \quad (3.12)$$

After some long calculations and using the previous stability conditions and limits, one gets  $|\zeta|^2 \leq 1$ , which proves the stability necessary condition. The third step is assuming that  $y^{(n+1)}$  depends only on  $y^{(n)}$ ,  $y^{(n-1)}$ , and  $y^{(n-2)}$  only. Then add the dependence on  $y^{(n-3)}$ , and so on till reaching  $y^{(0)}$ . At each step, one has to solve the resulted equation and the use of the previous limits, to get  $|\zeta|^2 < 1$ . So far the scheme is stable for the time-fractional order  $\beta$ . In the next section, we simulate the approximation solution of these models for different values of  $\beta$ ,  $k$ ,  $f(x)$  and for different  $t$ .

## 4 Stationary Continuous and Approximation Solutions

The stationary solution is the solution of the partial differential equations in the long run and is obtained by taking the limit as  $t \rightarrow \infty$  to the corresponding partial differential equation. Substitute  $F(x) = -bx$  and  $a = 1$  in equations (1.3) and (3.1), then take the limit at  $t \rightarrow \infty$ , then both equations go to the same partial differential equation, i.e. there is no dependence on  $t$ , namely

$$b \frac{\partial}{\partial x} x u(x) + \frac{\partial^2}{\partial x^2} u(x) = 0. \quad (4.1)$$

Regarding the initial condition, equation(4.1) has the solution

$$u(x) = \frac{1}{\sqrt{2\pi}} e^{-bx^2/2} = \frac{1}{\sqrt{2\pi}} e^{-U(x)}.$$

To find the stationary approximation solution of equations (1.3) and (3.1), we omit the dependence on the time  $t$  at equations (2.9) and (3.9). Both go to the same matrix equation  $z.H = 0$ , i.e.  $H^T.y = 0$ .  $H^T$  has an eigenvector  $y^*$  of eigenvalue zero. Our stationary approximation solution is  $\bar{y} = cy^*$  with  $c = 1 / \sum_{j=-R}^R y_j^*$  is a vector whose elements sum to 1. In what follows, we simulate these stationary solutions. We expect that the classical and the time-fractional all must have the same behavior on the long run.  $u(x)$  is simulated at figure[ 60] and its approximation solution is simulated at figure[ 61]. It is clear that the wave equation tends to the diffusion equation as  $t \rightarrow \infty$ .

## 5 Numerical Results and discussions

In this section, we give the numerical results of the approximation solution  $y^{(n)}$  of equation (1.4) for different values of the internal coefficient  $k$ ,  $\mu$ ,  $\beta$ ,  $t$  and for different initial functions  $f(x)$ . In our calculations, we take the function  $g(x) = 0$ . The values of  $h$  and  $\tau$  are related to the scaling relation  $\mu$  and to the value of the number of mesh points  $R$ . In these simulations we have enlarged the  $x$ -axis, as  $-20 \leq x \leq 20$  with  $h = 0.1$ . This large  $x$  dimension enables us to study the effect of the external and internal forces on the shape of the wave.

The first group of figures [ 1– 9] is plotted for fixing  $u(x, 0) = \sin(\frac{\pi x}{L})$ ,  $\mu = 0.25$ ,  $k = 1$ , and  $\beta = 2$ . This group of figures represents the time evolution of the classical case, and one can observe that the wave takes a long time,  $t = 65$ , till it reaches its stationary solution. This group also shows that the effect of the force is more effective than the effect of the internal force.

The second group of figures [ 10– 15] is plotted for the same initial conditions of the first group but with the time-fractional order  $\beta = 1.7$ . These figures represent the time evolution of the time-fractional damped forced wave. The figures shows that the effect of the internal force is much bigger than in the classical case and the effect of the memory enforces the wave to reach its stationary solution, at  $t = 19$ , i.e. much faster than the classical case.

The third group has the same initial conditions of the first group, but in this case we take  $k \leq 1$ , i.e.  $k = 0.5$ . We have the same start at  $t = 1$  and the model reaches its stationary solution also at  $t = 55$ . The figures [ 16– 21] shows that the effect of the damping coefficient  $k$  has not greater effect on the classical case.

The fourth group of figures [ 22– 27] is plotted with fixing the same initial conditions of the second group, i.e.  $\beta = 1.7$  but with  $k = 0.5$ . The model reaches its stationary solution at  $t = 25$ . This means that as  $k < 1$  the model is slower than as  $k = 1$ .

The fifth group, figures [ 28– 33], is plotted with same conditions of the third group but with  $\beta = 1.5$ . The model has the same start but reaches its stationary at  $t = 12$ , i.e. the stationary is slower than as  $k = 1$ .

In the next groups of figures, we change the scaling relation  $\mu = 0.5$  and the initial conditions of  $f(x)$ . Namely, we take  $f(x) = \delta(x)$ . We begin by the sixth group, figures[ 34– 42]. This group is simulated with  $\beta = 2$ , and  $k = 1$ . The model has the same start but it reaches its stationary at  $t = 58$ , i.e. it is faster than the first group of figures.

The seventh group, figures [ 43– 45], is compared with the second group as  $\beta = 1.7$  and  $k = 1$ . Here the model reaches its stationary at  $t = 20$ . Its behavior likes the second group.

The eighth group, figures [ 46– 51], is classical, i.e.  $\beta = 2$ , with  $f(x) = \delta(x)$  and  $\mu = 0.5$ , but  $k = 0.5$ , i.e. it is compared with the sixth group.

The ninth group of figures [ 52– 55] is simulated with the same  $f(x)$ ,  $k$  and  $\mu$  of the the first and second groups but with  $\beta = 1.5$ . The value of  $\beta$  is less than the second group. Therefore, the effect of the memory and the damping force is much bigger and that causes the wave to reach its stationary solution at  $t = 10$ .

The tenth group, figures [ 56– 59], is compared with the ninth group but here  $f(x) = \delta(x)$  and  $\mu = 0.5$ . The stationary state here is very fast, it is corresponding to  $t = 10$ .

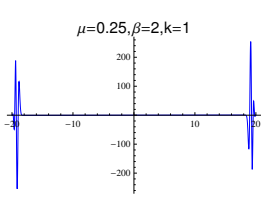


FIGURE 1.

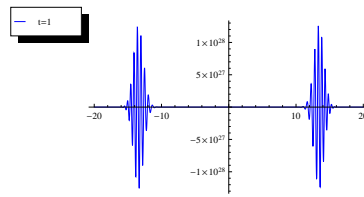


FIGURE 2.

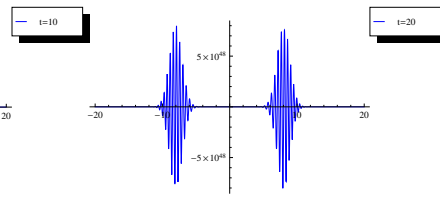


FIGURE 3.

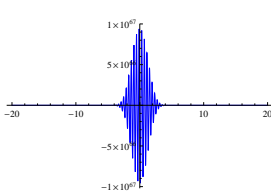


FIGURE 4.

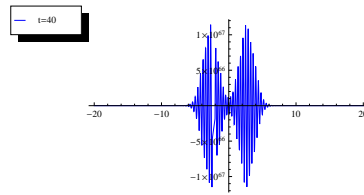


FIGURE 5.

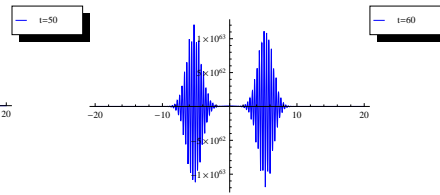


FIGURE 6.

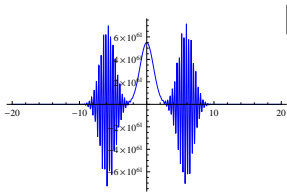


FIGURE 7.

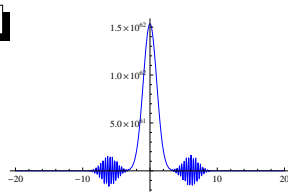


FIGURE 8.

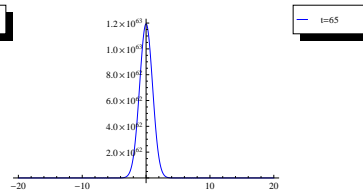


FIGURE 9.

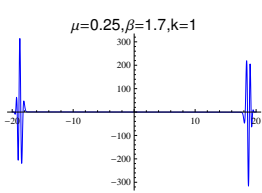


FIGURE 10.

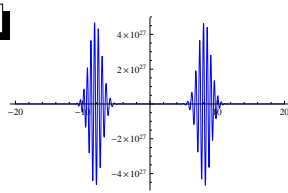


FIGURE 11.

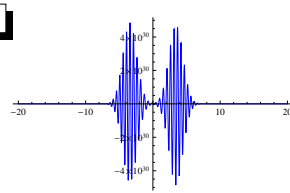


FIGURE 12.

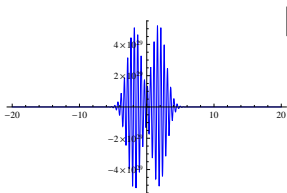


FIGURE 13.

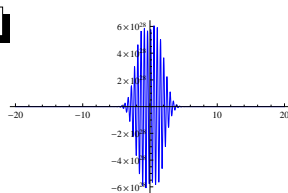


FIGURE 14.

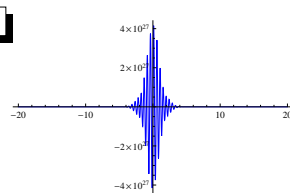


FIGURE 15.

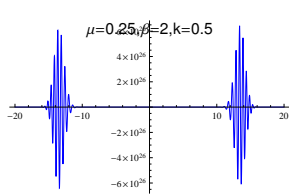


FIGURE 16.

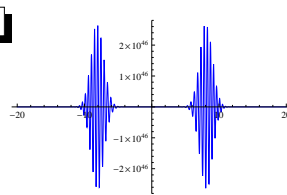


FIGURE 17.

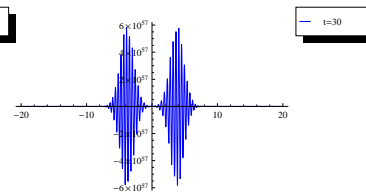


FIGURE 18.

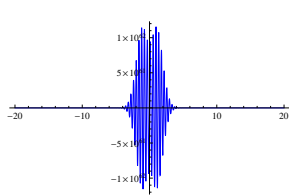


FIGURE 19.

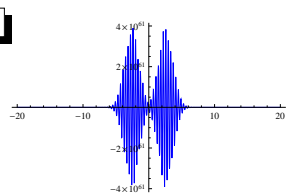


FIGURE 20.

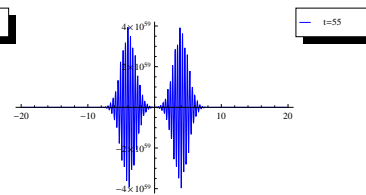


FIGURE 21.

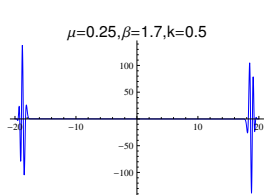


FIGURE 22.

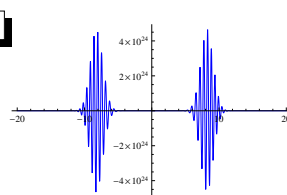


FIGURE 23.

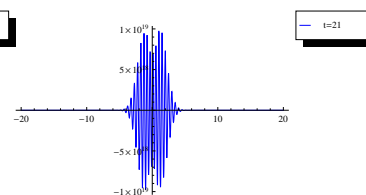


FIGURE 24.

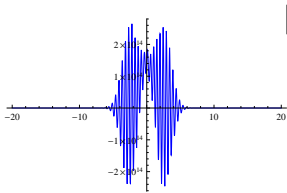


FIGURE 25.

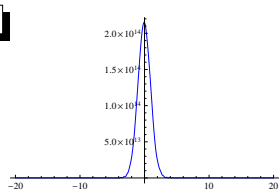


FIGURE 26.

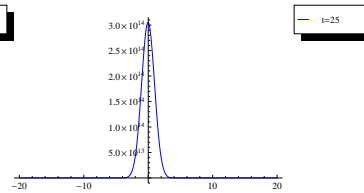


FIGURE 27.

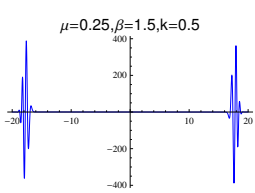


FIGURE 28.

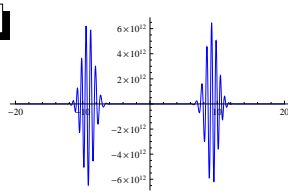


FIGURE 29.

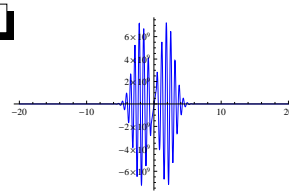


FIGURE 30.

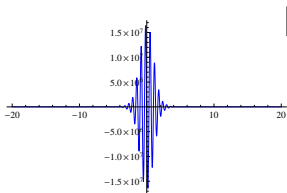


FIGURE 31.

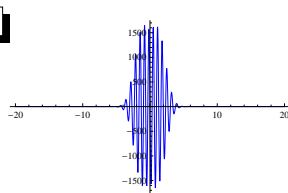


FIGURE 32.

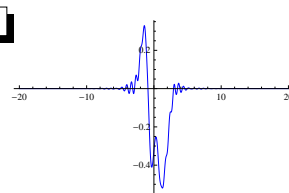


FIGURE 33.

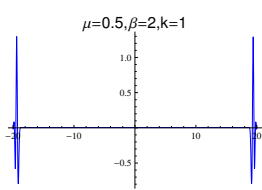


FIGURE 34.

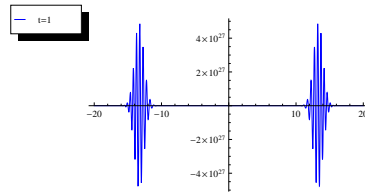


FIGURE 35.

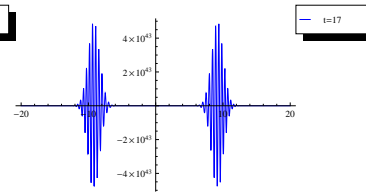


FIGURE 36.

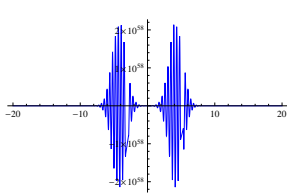


FIGURE 37.

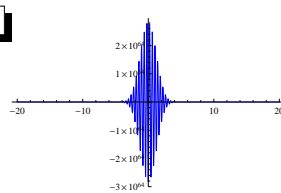


FIGURE 38.

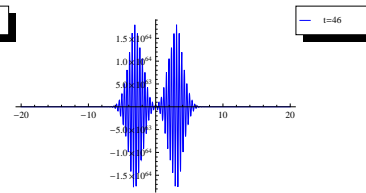


FIGURE 39.

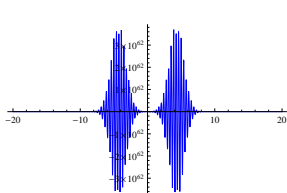


FIGURE 40.

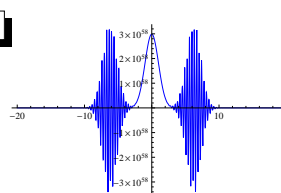


FIGURE 41.

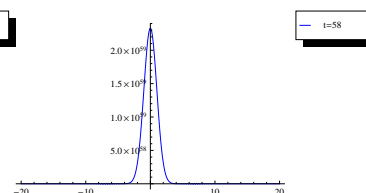


FIGURE 42.

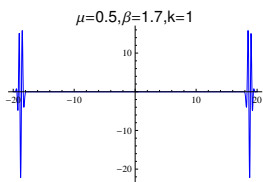


FIGURE 43.

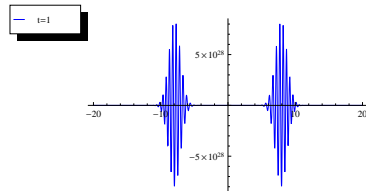


FIGURE 44.

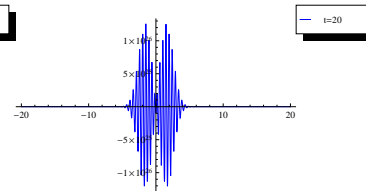


FIGURE 45.

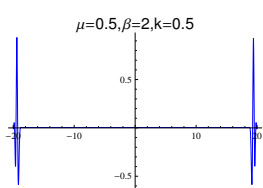


FIGURE 46.

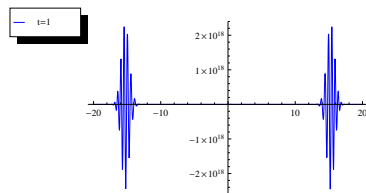


FIGURE 47.

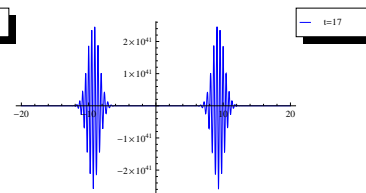


FIGURE 48.

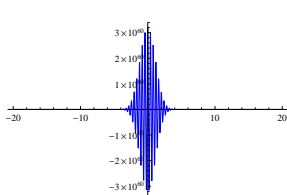


FIGURE 49.

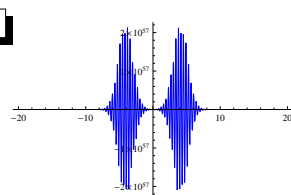


FIGURE 50.

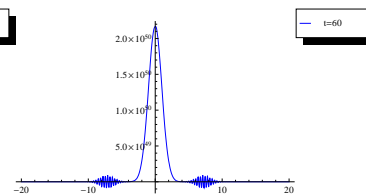


FIGURE 51.

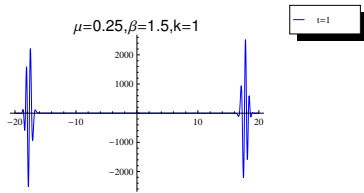


FIGURE 52.

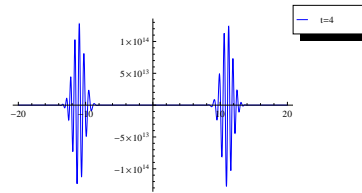


FIGURE 53.

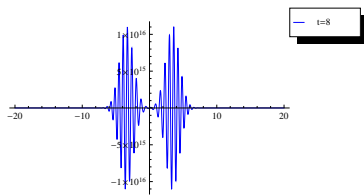


FIGURE 54.

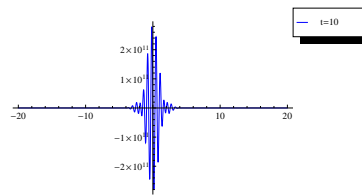


FIGURE 55.

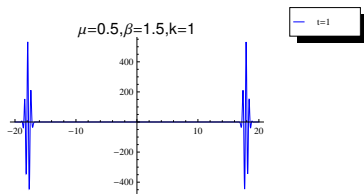


FIGURE 56.

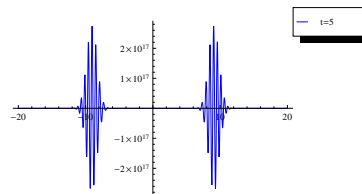


FIGURE 57.

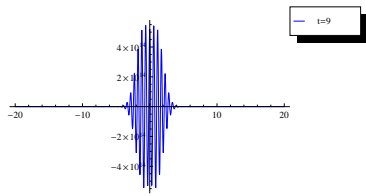


FIGURE 58.

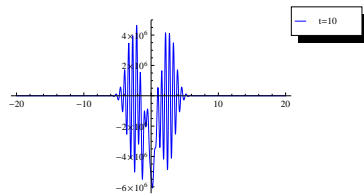


FIGURE 59.

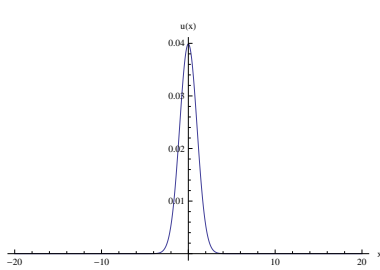


FIGURE 60.

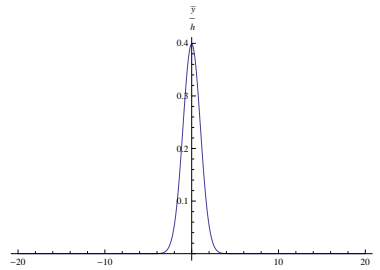


FIGURE 61.

## 5.1 Conclusion

We have studied numerically the time evolution of the approximation solution of the time–fractional–forced–damped–wave equation (1.4). We have plotted the approximation solutions for different values of  $\beta$ ,  $k$  and  $t$ . We have given also results for using the initial conditions  $u(x, 0) = \delta(x)$  and  $u(x, 0) = \sin(\frac{\pi x}{L})$ . The analytical stationary solution is also plotted and compared with the stationary approximation solution. The results show that the wave forced damped equation behaves exactly as the diffusion equation as  $t \rightarrow \infty$  which is expected.

## References

- [1] E. A. Abdel-Rehim, *Modelling and Simulating of Classical and Non-Classical Diffusion Processes by Random Walks* ( Mensch&Buch Verlag, 2004 ), ISBN 3–89820–736–6 Available at <http://www.diss.fu-berlin.de/2004/168/index.html>.
- [2] E. A. Abdel-Rehim, *Explicit Approximation Solutions and Proof of Convergence of the Space-Time Fractional Advection Dispersion Equations*, Scientific Research: Appl. Math. **4** (2013), 1427–1440.
- [3] E. A. Abdel-Rehim, *Implicit difference scheme of the space-time fractional advection diffusion equation*, J. Fract. Calc Appl. Anal. **18**, No. 6 (2015), 1252–1276.
- [4] O. P. Agrawal, *A general solution for the fourth-order fractional diffusion-wave equation*, J. Fract. Calc. Appl. Anal. **3**, No. 1 (2000), 1–12.
- [5] O. P. Agrawal, *Solution for a fractional diffusion-wave equation defined in a bounded domain*, J. Nonlinear Dynam. **29** (2002), 145–155.
- [6] R. C. Cascaval, E. C. Eckstein, C. L. Forta and J. A. Goldstein, *Fractional Telegraph Equations*, J. Math. Anal. Appl. **276**, No. 1 (2002), 145–159.
- [7] W. Chen, S. Holm, *Modified Szabós wave equation models for lossy media obeying frequency power-law attenuation*, J. Acoust. Soc. Am. **116** (2004), 2742–2750.
- [8] D. Constantinescu and M. Stoicescu, *Fractal dynamics as long range memory modelling techniques*, J. Physics. Auc. **21** (2011), 114–120.
- [9] M. Caputo, *Linear models of dissipation whose  $Q$  is almost independent II*, J. Geophys. Royal Astronom. Soc. **13** , No. 5 (1967), 529–539.
- [10] F. A. Duck, *Physical Properties of Tissue: A Comperhensive Reference Book*, Academic Press, Boston, 1990.
- [11] A. M. A. Elsayed, *Fractional-order diffusion and wave equation*, Int. J. Theor. Phys. **35** (1996), 311–322.
- [12] R. Gorenflo, A. Iskenderov and Y. Luchko, *Mapping Between Solutions of Fractional Wave Equations*, J. Fract. Calc. Appl. Anal. **3** (2000), 75–86.

- [13] R. Gorenflo, F. Mainardi, D. Moretti and P. Paradisi, *Time-fractional diffusion: a discrete random walk approach*, J. Nonlinear Dynam. **29** (2002), 129–143.
- [14] R. Gorenflo and E. A. Abdel-Rehim, *Discrete models of time-fractional diffusion in a potential well*, J. Fract. Calc. Appl. Anal. **8** (2005), 173–200.
- [15] M. A. E. Herzallah, A. M. A. Elsayed and D. Baleanu, *On the fractional-order diffusion-wave process*, Rom. J. Phys. **55** No. 3–4 (2010), 274–284.
- [16] J. K. Kelly, R. J. McGough and M. M. Meerschaert, *Analytical time-domain Green's functions for power-law media*, J. Acoust. Soc. Am. **124** (2008), 2861–2872.
- [17] V. Keyantuo, C. Lizama and M. Warma, *Asymptotic behavior of fractional order semilinear evolution equations*, J. Differ. Integral Equ. **26** No. 7–8 (2013), 757–780.
- [18] A. A. Kilbas, H. M. Srivastava and J. J. Trujillo, *Theory and Applications of Fractional Differential Equations*, Amsterdam, the Netherlands, 2006.
- [19] P. D. Lax and R. D. Richtmyer, *Survey of the stability of linear finite difference equations*, J. Comm. Pure Appl. Math. **IX** (1956), 267–293.
- [20] M. Liebler, S. Ginter, T. Dreyer and R. E. Riedlinger, *Full wave modeling of therapeutic ultrasound: Efficient time-domain implementation of the frequency power-law attenuation*, J. Acoust. Soc. Am. **116** (2004), 2742–2750.
- [21] C. Lizama, *Solutions of two-term fractional order differential equations with nonlocal initial conditions*, Electron. J. Qual. Theory Differ. Equ. **82** (2012), 1–9.
- [22] F. Mainardi, P. Paradisi, *Model of diffusive waves in viscoelasticity based on fractional calculus*, in Proceedings of the IEEE Conference on Decision and Control, **5**, O. R. Gonzales, IEEE, New York, 1997, pp. 4961–4966.
- [23] Y. Povstenk, *Signaling problem for time-fractional diffusion-wave equation in a half-plane*, J. Fract. Calc. Appl. Anal. **11** No. 3 (2008), 329–352.
- [24] H. M. Srivastava, R. K. Raina and X.-J. Yang, *Special Functions in a Fractional Calculus and Related Fractional Differential Equations*, Word Scientific–Imperial College Press, 2016.
- [25] M. Stojanovic, *Numerical method for solving diffusion wave phenomena*, J. Comp. Appl. Math. **2335** (2011) 3121–3137.
- [26] T. L. Szabo, *Time domain wave equation for lossy media obeying a frequency power law*, J. Acoust. Soc. Am. **96** (1994), 491–500.
- [27] Jin-Liang Wang and Hui-Feng Li, *Surpassing the fractional derivative: Concept of the memory-dependent derivative*, J. Comp. Math. with Appl. **62** (2011), 1562–1567.
- [28] X.-J. Yang, D. Baleanu and H. M. Srivastava, *Local Fractional Integral Transforms and Their Applications*, Academic Press (Elsevier Science Publishers), Amsterdam, Heidelberg, London and New York, 2016.